| Journal of Coastal Research | 14 | 2 | 483–492 | Royal Palm Beach, Florida | Spring 1998 |
|---|---|---|---|---|---|

# Sediment Geochronology in Changing Coastal Environments: Potentials and Limitations of the $^{137}Cs$ and $^{210}Pb$ Methods*

**G. Kirchner and H. Ehlers**

University of Bremen
Department of Physics/FB 1
D-28334 Bremen, Germany

**ABSTRACT**

KIRCHNER, G. and EHLERS, H., 1998. Sediment geochronology in changing coastal environments: Potentials and limitations of the $^{137}Cs$ and $^{210}Pb$ methods. *Journal of Coastal Research,* 14(2), 483–492. Royal Palm Beach (Florida). ISSN 0749-0208.

This paper describes the combined use of $^{137}Cs$ and $^{210}Pb$ radiotracers for obtaining information on sedimentation which in a changing coastal environment is subject to erosion, losses of sediments, and deposition of material that had been remobilized before from near-shore sediments in the course of storm surges. Geochronologies were established for sediment cores taken from salt marsh cliffs on the Isle of Sylt (Germany). Concentrations of $^{137}Cs$ and of excess $^{210}Pb$ were measured $\gamma$-spectrometrically. Micromorphological analyses of thin-sections showed that sediment mixing in all cores is negligible. An advection model was fitted to the vertical distributions of $^{137}Cs$. The results indicate that cores taken from sparsely vegetated areas had been denudated prior to sampling. This was confirmed independently by the lack of any Chernobyl-derived cesium in these cores. Taking denudation into account, $^{210}Pb$ geochronologies are consistent with sediment dating based on the $^{137}Cs$ data. Grain size analyses showed that only some sediment layers include a coarse sand fraction. The dating of these sandy layers coincides with periods of elevated storm surge activities, giving an independent validation of our method. We can conclude that sedimentation rates at the sites studied remained almost constant during the last 50 years. It is shown that capabilities and limitations of the $^{137}Cs$ and $^{210}Pb$ methods are complementary and that the combined use of both radiotracers is necessary for establishing reliable geochronologies in coastal environments.

**ADDITIONAL INDEX WORDS:** *Salt marsh geochronology, radiotracers, sedimentation rates, denudation.*

## INTRODUCTION

The present sea level rise that is generally attributed to global warming is likely to affect severely low-lying coastal areas around the world. Assessing this risk requires *inter alia* studying sediment fluxes in coastal areas and their changes with time. During the last decades $^{137}Cs$ and $^{210}Pb$ radiotracers have frequently been employed to determine recent sedimentation rates in lakes (*e.g.,* KRISHNASWAMY *et al.,* 1971; ROBBINS and EDGINGTON, 1975; STILLER and IMBODEN, 1986; ROBBINS and JASINSKI, 1995), in marine sediments (*e.g.,* KOIDE *et al.,* 1972; DOMINIK *et al.,* 1978; ABRIL *et al.,* 1992) and in accreting salt marshes (*e.g.,* DELAUNE *et al.,* 1978; LYNCH *et al.,* 1989; FRENCH *et al.,* 1994). Compared to these environments, coastal areas at risk from a rising sea level and from an increase of storm surges may show highly disturbed and incomplete sediment records: sedimentation processes may change with time and may be subject to episodic deposition events, erosion, losses of sediments, and deposition of material that had been remobilized before from near-shore sediments in the course of storm surges. To our knowledge only CLARKSON *et al.* (1983) established a geochronology of a rapidly changing coastal environment. They were able to identify storm surge deposits using $^{210}Pb$ dating, but noticed some disagreement with dates based on the $^{137}Cs$ measurements. Moreover, MILAN *et al.* (1995) recently questioned the applicability of the $^{137}Cs$ method for calculating sedimentation rates in coastal environments.

We investigated whether combining the information available from the distributions of $^{210}Pb$ and $^{137}Cs$ within the sediment sequence may provide consistent information on the sedimentation chronology in rapidly changing coastal areas. The island of Sylt, located in the German Bight of the North Sea, provides an ideal environment for this purpose because a rise in sea level and an increase of storm surges during this century have been previously documented. Thus, a second objective of this study is to establish the influence of these environmental changes on sedimentation and erosion processes at our experimental sites.

## STUDY AREA

The island of Sylt is one of the barrier islands along the Wadden Sea coast of the North Sea. The morphology and hydrology of the area are described in detail by EHLERS (1988). The mean tidal range at Sylt is about 1.7 m (STÄLEIN *et al.,* 1993). From gauge measurements along the German North Sea coast over the last 100 years a sea level rise of 0.2–0.3 cm $y^{-1}$ has been deduced (EHLERS, 1988). The frequency and

*96035 received 15 April 1996; accepted in revision 5 January 1997.*
**This work was supported by the Commission of the European Communities under contract EV5V-CT930266.*

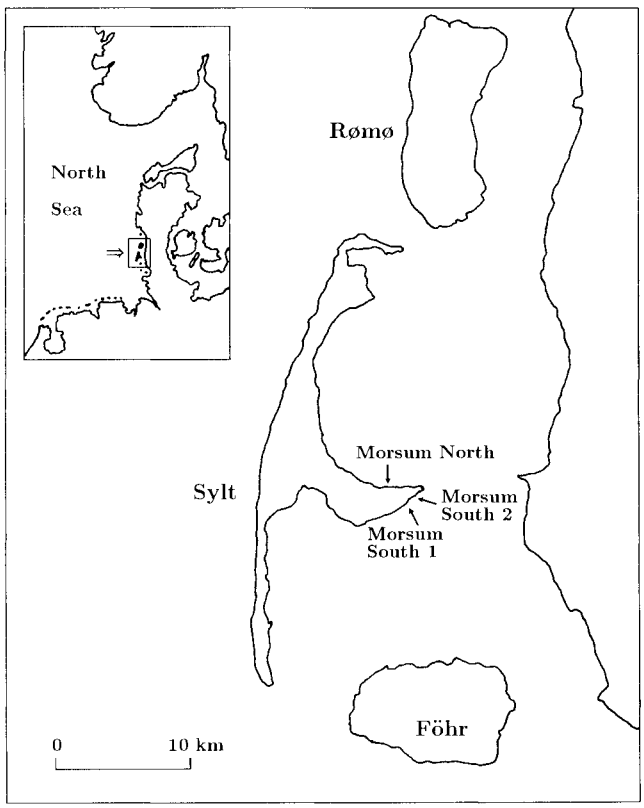


Figure 1. Location of the study areas.

intensity of storm surges in the Sylt area have both increased over the last 90 years (STÄBLEIN *et al.*, 1993).

Three experimental sites were chosen on undiked salt marshes (STÄBLEIN *et al.*, 1993). Two of these (Morsum South 1 and Morsum South 2) are situated on the southern coast, while the third (Morsum North) is on the northern coast of the Nösse Peninsula (Figure 1). Both coasts are retreating (STÄBLEIN *et al.*, 1993). The heights of the cliffs forming the coastlines vary between 20 and 110 cm. In the cliff profiles distinct layers are visible that indicate undisturbed sediment sequences. At Morsum North and Morsum South 2 great parts of the cliffs are covered by dense vegetation, whereas the cliff at Morsum South 1 is unvegetated. STÄBLEIN *et al.* (1993) estimate that these three sites, lying ca. 1.5 m above mean sea level, are flooded between 10 and 20 times per year.

## SAMPLING AND ANALYTICAL METHODS

Cores were taken near the tops of the cliffs in 1992. Two of the cores (MoSKF and MoSKG from Morsum South 2) were sliced into layers of 1 cm thickness, for the other two (MoSKB from Morsum South 1 and MoNK1 from Morsum North) coarser segmentations varying from 1 to 10 cm were chosen. For all samples grain size distributions were determined using standard procedures (GEE and BAUDER, 1986).

Thin-sections of the cores were prepared according to the technique described by CADY *et al.* (1986) and did not indicate any major redistribution within the sediment sequences. Furthermore, no compaction of deeper sediment layers was apparent.

$^{210}$Pb is traditionally determined by measuring α-spectrometrically its 138 d half-live decay product $^{210}$Po. This method requires laborious radiochemical separation techniques and long interim storage times to ensure that equilibrium between these two radionuclides has been attained. Therefore, we determined $^{210}$Pb γ-spectrometrically by measuring its 46.5 keV gamma line using a large volume Reversed Electrode High-Purity Germanium detector (Canberra, 55 % relative efficiency). Unlike conventional coaxial detectors, this detector has a useable energy range which extends below 50 keV (down to 5 keV). Activity concentrations of $^{226}$Ra were determined indirectly by utilizing the 352 keV γ-line of its decay product $^{214}$Pb, since the gamma decay energy of $^{226}$Ra (186 keV) interferes with a γ-line of $^{235}$U which may also be present in the sediments. Activity concentrations of $^{134}$Cs (604 keV), $^{137}$Cs (661.6 keV), $^{210}$Pb and $^{214}$Pb were simultaneously determined.

As the intensity attenuation of the low-energy rays of $^{210}$Pb within the sample considerably varies with changing densities of the sediment, 45 g of sediment were mixed with appropriate amounts of wax and pressed to pellets of standard geometry (70 mm diameter, 10 mm height) and density (1.5 g cm $^{-3}$). For this geometry and density the detector had been calibrated using a multi-isotope standard. The calibration uncertainty is below 5%. All samples were sealed prior to the measurements and stored for more than three weeks to ensure that $^{226}$Ra is equilibrated with its decay product $^{214}$Pb.

The reproducibility of the sample preparation was checked by preparing dublicates from some sediment layers. Taking into account the analytical uncertainties (detector calibration uncertainty and counting statistics), no differences between radionuclide concentrations of dublicate samples were detected.

## MODELS USED FOR DATING

### Cesium-137

$^{137}$Cs is a uniquely anthropogenic nuclear fission product. Since 1954 it is globally detectable in the environment as a result of atmospheric testing of atomic weapons. $^{137}$Cs in the North Sea originates from four main sources: (i) fallout of weapons testing, which peaked in 1963 and rapidly declined afterwards, (ii) emissions from the nuclear reprocessing plant at Sellafield (UK) with peak output between 1974 and 1978, (iii) emissions from the French reprocessing plant at Cap de La Hague, and (iv) fallout after the Chernobyl reactor accident in 1986. Annual means of concentrations measured in surface waters of the German Bight are shown in Figure 2. Cesium is strongly sorbed on fine particles, particularly clay minerals, silts and humic materials (STANNERS and ASTON, 1981; CUNDY and CROUDACE, 1995; MILAN *et al.*, 1995). Therefore, activity concentrations for each sample were normalized to the sum of the mineral fraction with grain size $<20$ μm and the organic fraction (ACKERMANN *et al.*, 1983).

Sediment accumulation rates are traditionally calculated by relating the first occurrence of $^{137}$Cs in the sediment se-

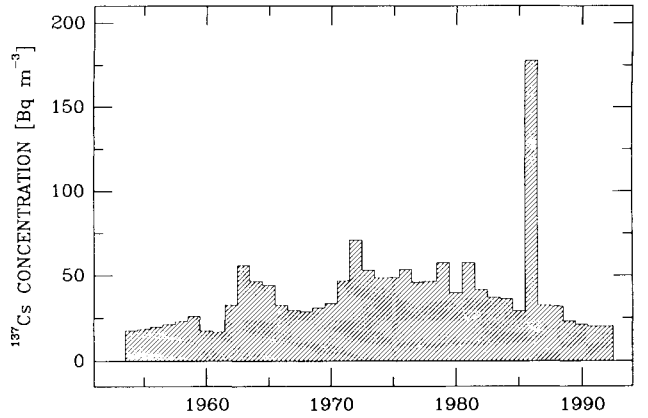


Figure 2. $^{137}$Cs concentrations in surface waters of the German Bight. Data taken from the compilation by BAUMANN (1991) and from annual monitoring reports (BMU, undated).

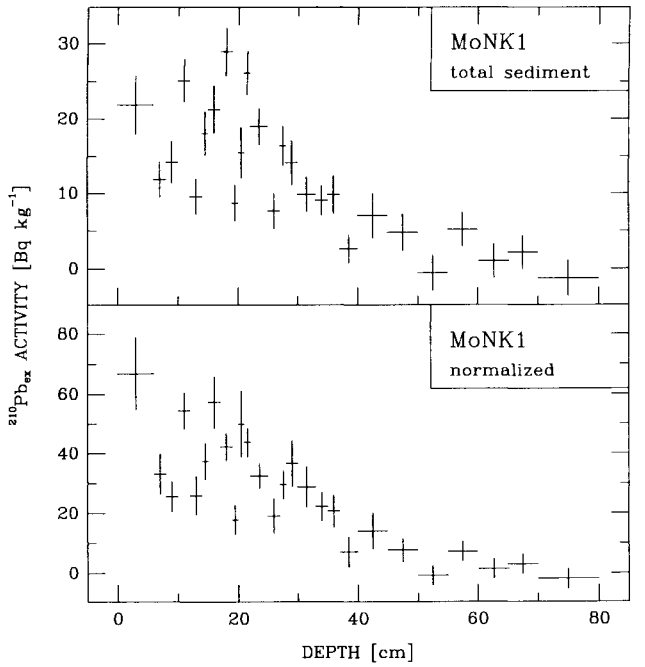


Figure 3. Distribution of excess $^{210}$Pb in core MoNK1. Top: activity concentrations per kg of bulk sediment, bottom: data normalized to the organic fraction plus the mineral fraction of <20 μm grain size of the samples. Error bars denote the sample thickness horizontally and one standard deviation of the activity including counting statistics and detector calibration uncertainty vertically.

quence to the year 1954 and its maximum activity to 1963 (*e.g.*, DELAUNE *et al.*, 1978; DOMINIK *et al.*, 1978; CHANTON *et al.*, 1983; LYNCH *et al.*, 1989). The small amounts initially present in 1954 may no longer be detectable. The main shortcoming of basing a sediment geochronology on a few point markers is that it makes only little use of the information on sedimentation processes which is stored in the $^{137}$Cs distribution in the sediment sequence. In particular, changes of sedimentation rates with time can not be identified only from a few datums.

Particle-associated tracers are transported within the sediment column by sediment accumulation as well as by sediment mixing. Particle mixing often is assumed to be analogous to eddy diffusion, with tracer displacement within the sediment column being described by the diffusion-advection equation as first proposed by GOLDBERG and KOIDE (1962). If particle mixing and sediment compaction are negligible (see above), this equation simplifies to

$$\frac{\partial C(x, t)}{\partial t} = -S\frac{\partial C(x, t)}{\partial x} - \lambda C \qquad (1)$$

where $C$ is the $^{137}$Cs activity concentration in the sediment (Bq kg$^{-1}$), $x$ is the depth measured from the top of the sediment core (cm), $S$ is the sedimentation rate (cm y$^{-1}$) and λ is the radioactive decay constant (y$^{-1}$). For the initial condition $C(x, 0) = 0$ and a time independent sedimentation rate, eqn. (1) has the simple solution

$$C(x, t) = I_0(\theta)\exp\left(-\frac{\lambda}{S}x\right) \qquad (2)$$

where $I_0$ is an arbitrary time-dependent input function (Bq kg$^{-1}$) of the parameter $\theta = t - x/S$. Cesium in sea water becomes attached to inorganic particles by ion exchange resulting in a dynamic equilibrium between the Cs in water and on suspended particulates (DUURSMA and EISMA, 1973; OLSEN *et al.*, 1982). In the following, the cesium loading of particulate matter at the time of sedimentation is assumed to be proportional to the mean annual concentration in sea water. Thus, the input function $I_0$ is constant within each year:

$$I_0(t) = K_s C_i^0 \text{ for } (i - 1)\Delta t < t \leq i\Delta t,\ i = 1, \ldots, N \qquad (3)$$

where $\Delta t = 1$ year, $K_s$ is the water-particulate distribution coefficient (m$^3$ kg$^{-1}$), $C^0_i$ (Bq m$^{-3}$) are the mean annual concentrations of $^{137}$Cs in sea water as shown in Figure 2, and $N$ is the number of years since $^{137}$Cs was detected in sea water for the first time (i.e., 1954).

Sectioning of the sediment cores will generate samples which are comprised of sediments deposited in several years. Cesium concentrations in such samples will be the average of the annual deposits included in the analysed core sections. Using eqns. (2) and (3) we obtain

$$C(\Delta x, t) = K_s \sum_{m=j}^{k} f_m C^0_{N-m}\exp(-\lambda\tau_m) \qquad (4)$$

where $\Delta x = x_{i+1} - x_i$ is the length of the core section. The indices $j$, $k$ are given as

$$j = \text{Int}\left(\frac{x_i}{S\Delta t}\right) + 1, \qquad k = \text{Int}\left(\frac{x_{i+1}}{S\Delta t}\right) + 1 \qquad (5)$$

where Int denotes the integer part function. The fraction $f_m$ each annual layer contributes to a distinct core section $\Delta x$ is

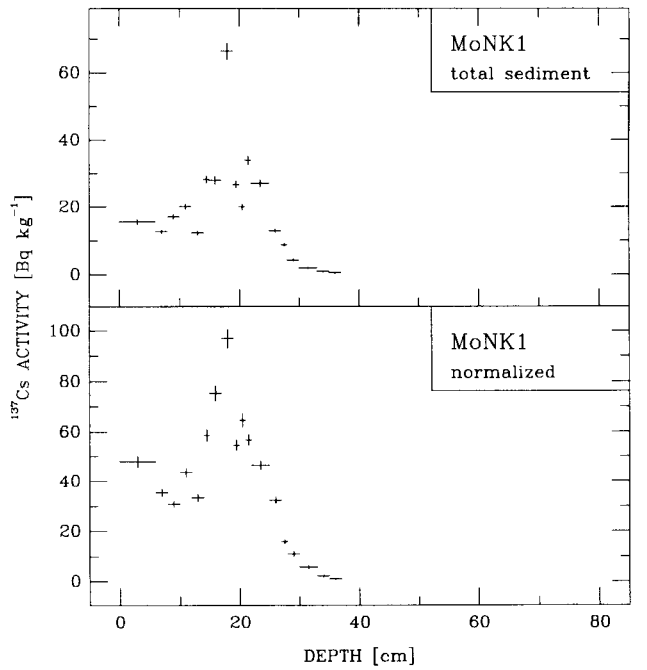


Figure 4. Distribution of $^{137}$Cs in core MoNK1. Top: activity concentrations per kg of bulk sediment, bottom: data normalized to the organic plus <20 μm mineral fractions of the samples. Error bars are as in Figure 3.

$$f_m = \begin{cases} m - \dfrac{x_j}{S\Delta t} & m = j \\ 1 & j < m < k \\ \dfrac{x_{j+1}}{S\Delta t} - (m - 1) & m = k \end{cases} \quad (6)$$

with mean times after deposition $\tau_m$ of those fractions

$$\tau_m = \begin{cases} (m - 0.5f_m)\Delta t & m = j \\ (m - 0.5f_m)\Delta t & j < m < k \\ (m - 1 + 0.5f_m)\Delta t & m = k \end{cases} \quad (7)$$

An algorithm based on eqns. (4) to (7) was developed and built into the nonlinear regression code PAR of the BMDP statistical code package (DIXON, 1990). Using $K_s$ and $S$ as free parameters, this model was fitted to the vertical distribution of $^{137}$Cs in a core. Since the cores were taken from the tops of the coastal cliffs, we can not exclude that part of the sediment sequence had been denudated (e.g., due to storm surges) prior to sampling. To test this, fitting was performed repeatedly for each core with the $x$-coordinate shifted by an increment $\delta x$ which was varied until the best fit was obtained.

## Lead-210

$^{210}$Pb is produced in the atmosphere by the decay of gaseous $^{222}$Rn and reaches the sea surface by precipitation scavenging. In coastal marine waters it readily adsorbs to suspended particles (SCHELL, 1977) which may be incorporated in the sediments. This 'unsupported' or 'excess' $^{210}$Pb decays to the

Table 1. *Sedimentation rates and denudations calculated for the various cores; for explanation of the uncertainties stated, see text.*

| Core | Sedimentation Rate [cm y$^{-1}$] $^{137}$Cs | Sedimentation Rate [cm y$^{-1}$] $^{210}$Pb | Denudation (cm) |
|---|---|---|---|
| MoNK1 | 0.92 ± 0.02 | 0.94 ± 0.19 | 0 ± 0.5 |
| MoSKB | 1.52 ± 0.04 | 1.20 ± 0.22 | 7 ± 0.5 |
| MoSKF | 1.28 ± 0.02 | 1.15 ± 0.19 | 13 ± 0.5 |
| MoSKG | 1.02 ± 0.01 | 0.58 ± 0.06 | 16 ± 0.5 |

background value produced by its long-lived precursor $^{226}$Ra in the sediment. Concentrations of the 'supported' $^{210}$Pb are usually low compared to those of excess $^{210}$Pb; however some exception has been reported (STILLER and IMBODEN, 1986). Like Cs, Pb is preferentially sorbed to clay minerals, fine silts and humic materials (BENNINGER and KRISHNASWAMI, 1981; OLSEN *et al.*, 1982; CHANTON *et al.*, 1983; CUNDY and CROUDACE, 1995). Therefore, activity concentrations of lead in each sample were also normalized to the sum of the mineral fraction of <20 μm grain size and the organic fraction (ACKERMANN *et al.*, 1983). Excess $^{210}$Pb was calculated by subtracting $^{214}$Pb activity concentrations measured in equilibrium with $^{226}$Ra from $^{210}$Pb activity concentrations.

The use of $^{210}$Pb for sediment geochronologies is based on observations showing that annual deposition of excess $^{210}$Pb from the atmosphere is relatively constant (TUREKIAN *et al.*, 1977; RANGARAJAN *et al.*, 1986). As a consequence, it is reasonable to assume constant concentrations of excess $^{210}$Pb in sea water and on suspended particles. If mixing processes and compaction within the sediment core can be disregarded (for our cores this was confirmed by thin-section analyses, see above), and if additionally the sedimentation rate is assumed

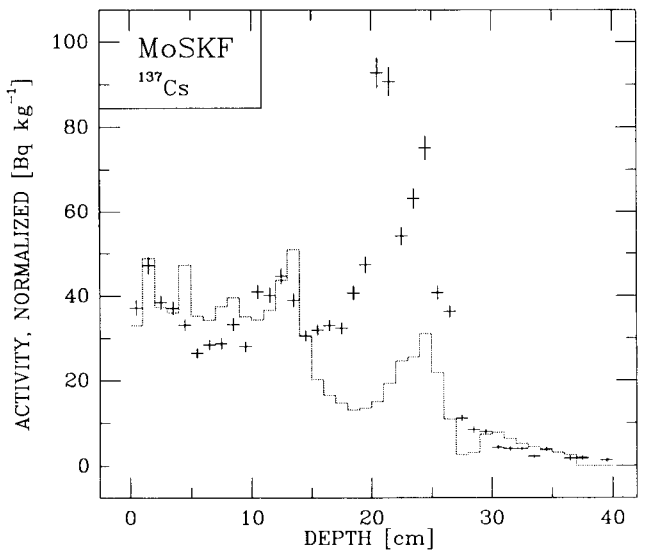


Figure 5. Fit of the $^{137}$Cs model (dotted line) to the measured activity distribution (data points) in core MoSKF. The error bars of the experimental data have the same meaning as in Figure 3.

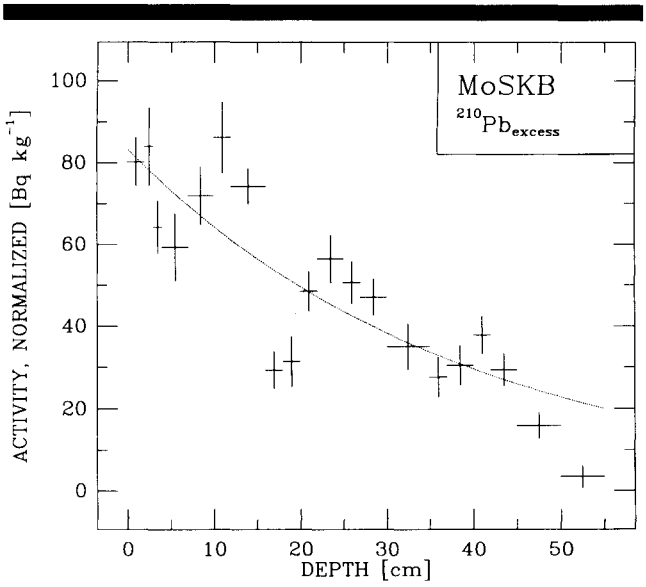


Figure 6. Fit of the c.i.c. model (dotted line) to the activity distribution of excess $^{210}$Pb measured in core MoSKB. Error bars are as in Figure 4.

not to vary with time, the concentration of excess $^{210}$Pb, $C_{ex}$, at depth $x$ is given by (KRISHNASWAMY *et al.*, 1971)

$$C_{ex}(x) = C_{ex}^{0}\exp\left(-\frac{\lambda}{S}x\right) \quad (8)$$

where $C_{ex}^{0}$ is the concentration of excess $^{210}$Pb in the sediment at the time of deposition (Bq cm $^{3}$). This model often is referred to as the 'constant initial concentration (c.i.c.)' model. Eqn. (8) corresponds to the solution of eqn. (1) for steady-state conditions. APPLEBY and OLDFIELD (1978) were the first to propose the 'constant rate of supply (c.r.s.)' model which accounts for varying sedimentation rates. In this model the age $t_x$ of a sediment at depth $x$ is

$$t_x = \frac{1}{\lambda}\ln\frac{\int_0^{x} C_{ex}(x')\,dx'}{\int_l^{\infty} C_{ex}(x')\,dx'}. \quad (9)$$

Using $C_{ex}^{0}$ and $S$ as free parameters, eqn. (8) was fitted to the vertical distribution of excess $^{210}$Pb in a core. The nonlinear regression code PAR of the BMDP statistical code package (DIXON, 1990) was used again. A successful fit to the experimental data is interpreted as suggesting that the underlying assumption of a constant sedimentation rate holds.

## RESULTS AND DISCUSSION

### Grain Size Effects

As a typical example, raw excess $^{210}$Pb activities of bulk sediments of the MoNK1 core show large fluctuations and in parts of the sediment column hardly any variation with depth is apparent (Figure 3; top). Normalizing the lead activities to the sum of the organic fraction and the mineral fraction of <20 μm grain size of the sediment samples (Fig. 3; bottom) records an exponential decline with depth as predicted theoretically (see eqn. (8)), although some scattering (discussed below) is still apparent.

For the same core, no cesium was detected below 36 cm depth (Figure 4). In the uppermost part of the core (0–6 cm) the Chernobyl-specific isotope $^{134}$Cs was detected. If activities are normalized to the sum of the organic and the <20 μm grain size mineral fraction of the sediment samples (bottom panel), the elevated cesium input due to the Chernobyl accident becomes apparent in terms of Cs flux.

### Sedimentation Rates Based on $^{137}$Cs

Using the cesium transport model described above, we obtained the sedimentation rates and denudations given in Table 1. Uncertainties given for the sedimentation rates denote their asymptotic standard deviations. The uncertainties of the denudations were estimated taking into account (i) the difficulties in exactly localizing the uppermost sediment layer in the plant rooting zone if the sediment was vegetated, and (ii) the uncertainty due to shifting the $x$-coordinate in 1 cm steps when testing for denudation. The sedimentation rates calculated are in good agreement between the 4 cores with a mean of *ca.* 1 cm per year. For MoSKF and MoSKG, the cesium data indicate considerable denudation. This result is supported by the fact that no $^{134}$Cs was detected in either sediment column. This isotope, which has a half-live of 2.04 years, was initially present in the Chernobyl fallout with an $^{134}$Cs:$^{137}$Cs activity ratio of 0.528 ± 0.008 (KIRCHNER and NOACK, 1988). $^{137}$Cs concentrations in the uppermost samples of these two cores were high enough to have allowed detection of $^{134}$Cs if the cesium in these samples had come from the Chernobyl accident. One potential explanation for the enhanced denudation at these sites may be that both sites are more sparsely covered by vegetation than the Morsum North site (MoNK1), for which no denudation is apparent.

As an example, for the MoSKF core the model matches the overall measured trend quite well, but deviations are apparent (Figure 5). Partially they may be caused by the assumption made (eqn. 3) that cesium loadings of particulate matter at the time of sedimentation correspond to the mean annual concentrations in sea water. Cesium concentrations in waters of the German Bight often showed large fluctuations within one year (BMU, undated). As concentrations attached to suspended particulates closely follow concentrations in sea water, actual $^{137}$Cs concentrations of sediment deposited in a single event (*e.g.*, during a storm surge) could differ considerably from concentrations calculated based on annual means. However, since no data are available on short term fluctuations of cesium concentrations in sea water in the area of the island Sylt, using annual mean values seems to be the most reasonable approach.

Concentrations of the cesium peak at about 20 cm depth are clearly underpredicted (Figure 5). This discrepancy is seen similarly for all cores analyzed. A reasonable explanation is given by the fact that in our model direct atmospheric deposition of $^{137}$Cs is not taken into account. As our sampling sites are flooded by high tides only, this atmospheric pathway

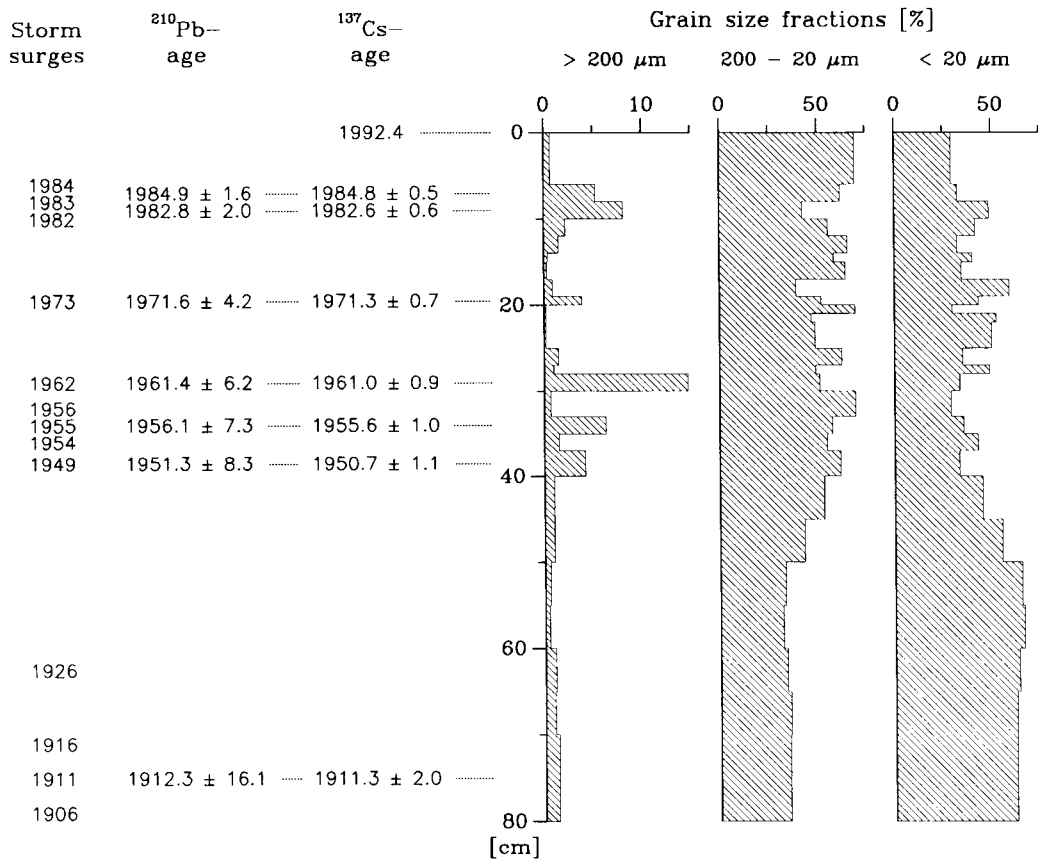


Figure 7. Grain size distributions of the samples of core MoNK1, $^{137}Cs$ and $^{210}Pb$ ages of samples enriched in coarse material and years of elevated storm surge activity; uncertainties of the geochronologically derived dates denote one standard deviation.

has contributed significantly to cesium loading of the sediments during the time period of high concentrations of $^{137}Cs$ in the atmosphere around 1963. From the depth distribution in soils in Northern Germany, a mean deposition of 3000 Bq $m^{-2}$ of nuclear weapons fallout $^{137}Cs$ is deduced of which *ca.* 50% were deposited between 1963 and 1965 (KIRCHNER and BAUMGARTNER, 1992). With mean bulk densities of our sediments of *ca.* 1.25 g $cm^{-3}$ this corresponds to 125 Bq cm $kg^{-1}$ $^{137}Cs$ (*ca.* 250 Bq cm $kg^{-1}$ after grain size correction) of atmospheric origin. Taking radioactive decay into account, this figure is in good agreement with the peak area not accounted for by our model (Figure 5).

In addition, the benefit of using the somewhat more sophisticated model of eqns. (4) to (7) rather than basing the interpretation simply on the location of cesium peaks in the sediment column is clearly shown (Figure 5): in the usual approach the occurrence of some denudation could be inferred from the lack of any Chernobyl peak. However, to quantify its extent and, as a consequence, to calculate any sedimentation rate for these cores would be impossible.

## Sedimentation Rates Based on $^{210}Pb$

Considering their asymptotic standard deviations, sedimentation rates calculated from the excess $^{210}Pb$ activity concentrations using the c.i.c. model (eqn. (8)) are in good agreement with sedimentation rates calculated from the $^{137}Cs$ data for three of the four cores analyzed (Table 1). This correspondence between the results of two independent methods gives additional credit to the suitability of both techniques. For the MoSKG core, however, significantly different sedimentation rates were calculated by the two radiotracer methods. Since the depth distributions of both radionuclides were reasonably well fitted by the employed models, neither can be excluded.

The excess $^{210}Pb$ exponentially declines with depth as predicted by eqn. (8), thus confirming the applicability of the c.i.c. model (Figure 6). However, similarly to the other three cores, the scattering of the $^{210}Pb$ concentrations we find is much higher than reported for lacustrine (*e.g.*, Robbins and EDGINGTON, 1975) and marine (*e.g.*, KOIDE *et al.*, 1972) sediments. This may reflect the greater variability of both the processes and the type of particulate matter contributing to the accretion of sediments in a rapidly changing coastal environment. In addition, part of this scattering may be caused by temporal variations of $^{210}Pb$ in the atmosphere (JAWOROWSKI *et al.*, 1978; RANGARAJAN *et al.*, 1986).

The contribution of direct atmospheric deposition to the measured excess $^{210}Pb$ can be estimated as follows: NIJAMPURKAR and RAO (1993) report a mean annual deposition of

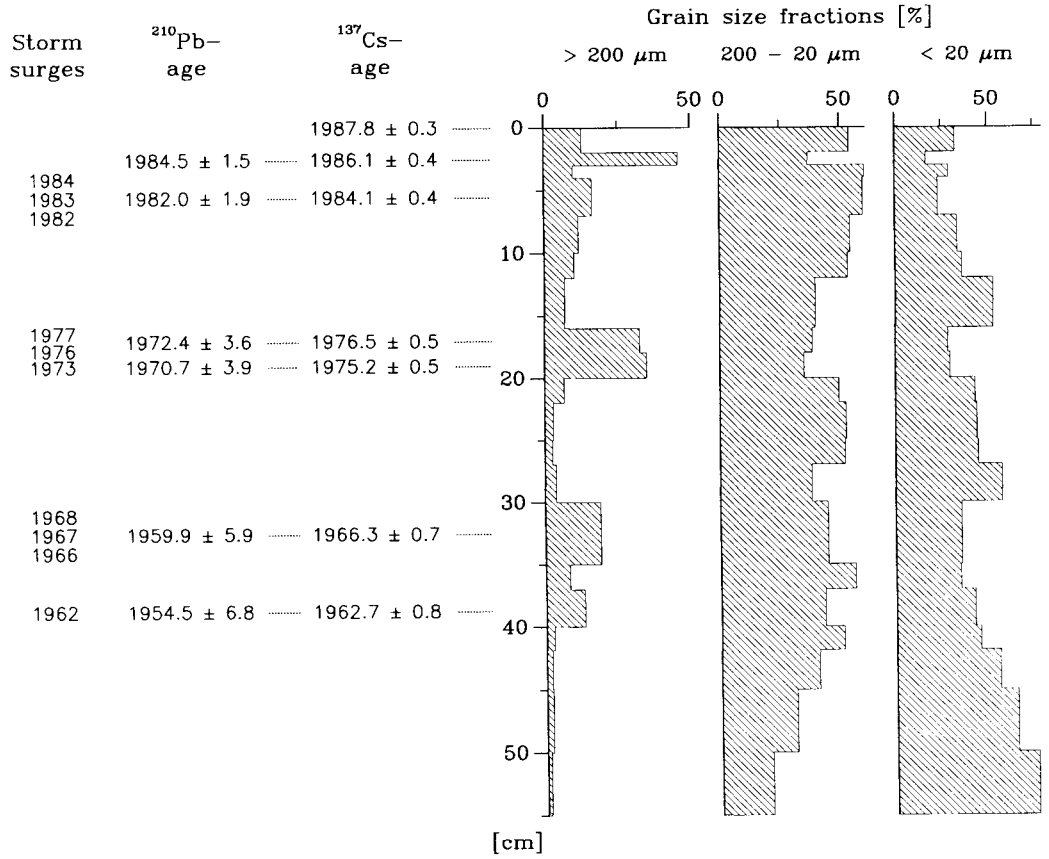


Figure 8. Grain size distributions of the samples of core MoSKB, $^{137}$Cs and $^{210}$Pb ages of samples enriched in coarse material and years of elevated sturm surge activity; uncertainties of the geochronologically derived dates denote one standard deviation.

3.67 mBq cm $^{-2}$ y $^{-1}$ in the 30–60°N latitude belt. Assuming steady state conditions, this implies a total $^{210}$Pb inventory of 0.12 Bq cm $^{-2}$ in a sediment or soil column. Bulk densities of our sediments are ca. 1.25 g cm $^{-3}$, resulting in a steady state excess $^{210}$Pb inventory of 95 Bq cm kg $^{-1}$ in the sediment sequence. The inventories which we measured in our sediments are always by more than a factor of 8 larger than this amount (*e.g.*, Figure 3), showing that lateral transport of $^{210}$Pb attached to particulate matter dominates at these sites. The global figure given by NIJAMPURKAR and RAO (1993) is in good agreement with the $^{210}$Pb regime in our study region: concentrations of $^{210}$Pb measured in rain water in Germany are in the range of 20–100 Bq liter $^{-1}$ (BMU, undated); with a mean precipitation of 700 mm y $^{-1}$ this results in annual depositions of 1.4–7.0 mBq cm $^{-2}$ y $^{-1}$. It should be noted that direct atmospheric deposition of $^{210}$Pb does not limit the applicability of eqn. (8) as long as residence times of $^{210}$Pb in coastal waters are low.

Application of the c.r.s. model (eqn. 9) to the $^{210}$Pb data of these cores is impossible. The reason is apparent from Figure 6: Concentrations of Pb-210 are exceptionally low between 15 to 19 cm depth. Since sediment dating indicates that these layers are storm surge deposits (see below), a reasonable explanation is that these are aged sediments which had been remobilized in the course of a storm surge and subsequently redistributed. Such a process, however, violates the basic assumption of the c.r.s. model that every deviation of the excess $^{210}$Pb from a strictly exponential decline with depth is due to a variation in the sedimentation rate.

It should be noted that capabilities and limitations of the $^{137}$Cs and $^{210}$Pb methods are complementary: In contrast to the $^{137}$Cs data, no information on denudation is available from the $^{210}$Pb profile. On the other hand, any hiatus in the sediment sequence is easily apparent as a sharp step in the $^{210}$Pb distribution with depth (ROBBINS *et al.*, 1978), but would be difficult to be detected from the cesium data. As a consequence, only the *combined* use of both radiotracers is likely to give reliable estimations of sedimentation rates in coastal environments.

## Sediment Geochronologies

Using the sedimentation and denudation data from Table 1, geochronologies of the analyzed sediment cores were established (Figures 7 to 10). For the $^{210}$Pb geochronologies the denudation derived from the corresponding $^{137}$Cs distribution with depth was taken into account. For comparison, phases

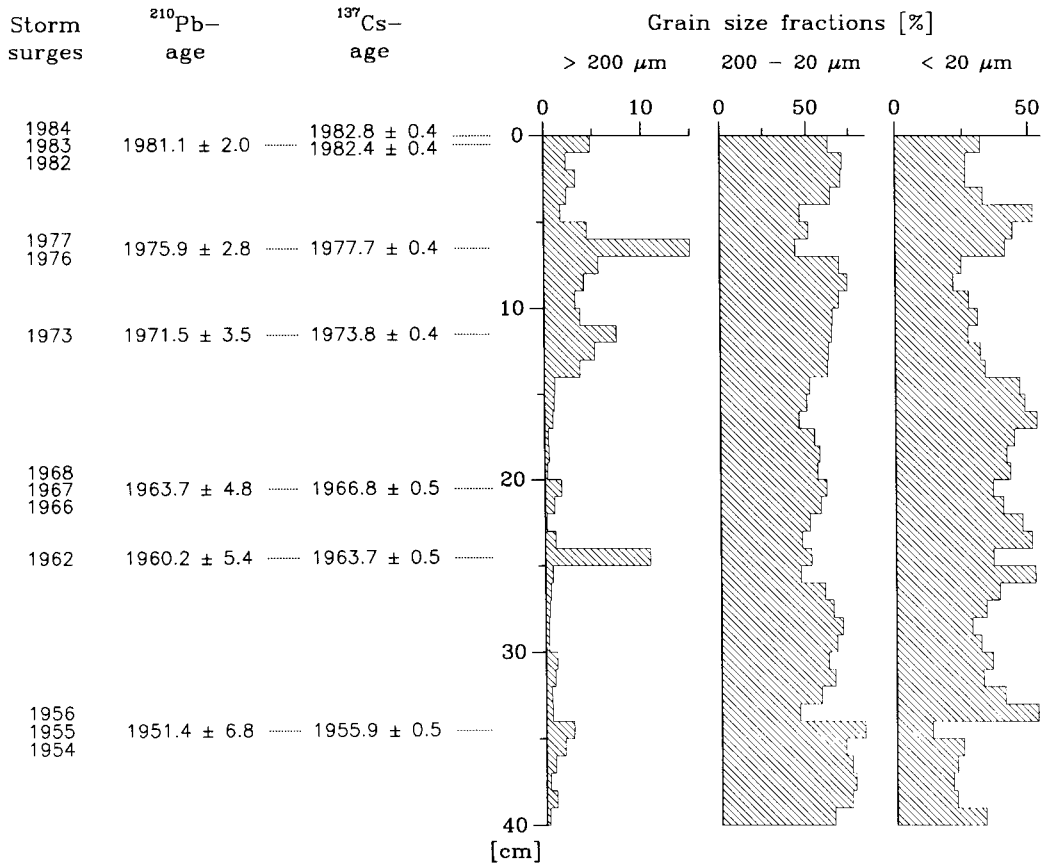


Figure 9. Grain size distributions of the samples of core MoSKF, $^{137}$Cs and $^{210}$Pb ages of samples enriched in coarse material and years of elevated sturm surge activity; uncertainties of the geochronologically derived dates denote one standard deviation.

of elevated storm surge activities in the Sylt area (EHLERS, 1988; STÄBLEIN *et al.*, 1993) are listed.

For three of the four cores (MoNK1, MoSKB, MoSKF), some of the samples show elevated fractions of coarse sands (>200 μm grain size). Both the $^{137}$Cs and the $^{210}$Pb geochronology indicate that these layers correspond to years in which high storm surge activities have been recorded (Figures 7 to 9). This confirms results reported by CHANTON *et al.* (1983) who in rapidly accreting coastal sediments found a number of distinct sand layers and interpreted these as storm surge traces by using a $^{210}$Pb geochronology. Even elevated fractions of coarse material which are barely apparent from a visual inspection of the sediment core may indicate storm surge deposits (Figure 7). This result could be particularly useful if sedimentation rates are low, since identification of storm surge traces will be possible without the need of choosing very fine segmentation of a sediment core—a conclusion which is confirmed by our success in identifying storm surge deposits in the MoNK1 and MoSKB cores partially sliced in quite coarse segments (Figures 7, 8).

The close agreement of the $^{137}$Cs dates of the sand-rich sediment samples in these three cores with known periods of elevated storm surge activities in the study area is remarkable. It confirms the applicability of our simple $^{137}$Cs sedimentation model in spite of the deviations of its fits from the measured concentrations (see Figure 5 and discussion above). Taking into account their asymptotic standard deviations, $^{210}$Pb derived ages of the sand-rich layers are in good agreement with their corresponding $^{137}$Cs ages and with years of elevated sturm surge activity. The larger uncertainties of the $^{210}$Pb geochronology reflects the scattering of the excess $^{210}$Pb in the cores analyzed (Figure 6).

Core MoSKG taken from Morsum South 2 is exceptional: Not only is there disagreement between the sedimentation rates calculated by the two radionuclides, but the sediment sequence does not show any marked layers enriched in coarse material (Figure 10). As a consequence, no reasonable geochronology could be established for this core. We plan to resample this area in order to decide whether the results given here are an artefact or reflect sediment deposition processes which violate basic assumptions of the employed models.

All geochronologies shown in Figures 7 to 9 are based on models which assume constant sedimentation rates. Their good agreement with the sturm surge records indicates that the sedimentation regime in this area has not changed significantly during the last ca. 45 years despite of the increase in both frequency and intensity of storm surges during this time period, as documented by STÄBLEIN *et al.* (1993). The

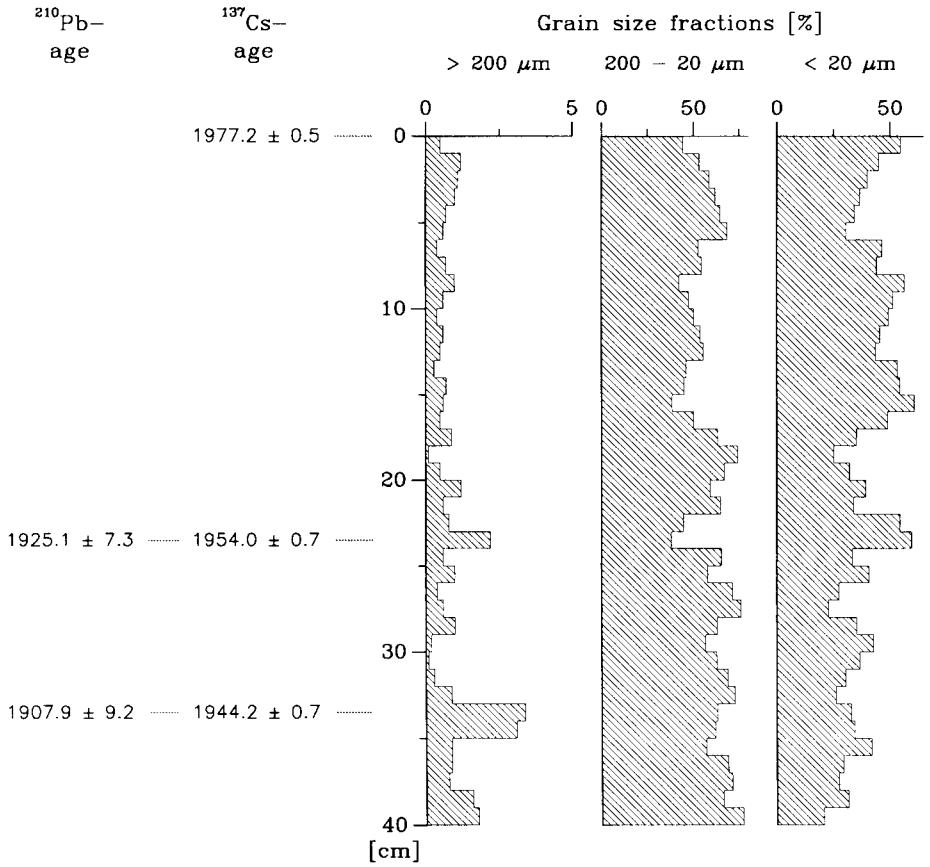


Figure 10. Grain size distributions of the samples of core MoSKG and $^{137}$Cs and $^{210}$Pb ages of samples enriched in coarse material; uncertainties of the geochronologically derived dates denote one standard deviation.

success in tracing back storm surge deposits in core MoNK1 to the beginning of this century might suggest that sedimentation rates remained constant even for more than 70 years—but without confirmation by additional evidence this conclusion must be taken with caution.

## CONCLUSION

The present study shows that by using the distribution with depth of both $^{137}$Cs and $^{210}$Pb it is possible to date recent sediments in rapidly changing coastal environments. Activity concentrations measured always must be corrected for grain size effects. Since capabilities and limitations of information available from these two radiotracers are complementary in many respects, both methods have to be combined in order to identify processes such as denudation, hiatus, varying sedimentation rates and deposition of aged coastal sediments after remobilization. Thin-sections give valuable information on the extent of sediment mixing and compaction, and they supplement the radiotracer methods. Interpretation of the $^{137}$Cs data should be based on a suitable transport-sedimentation model in order to fully utilize the information available from the $^{137}$Cs distribution in the sediment sequence and to avoid misinterpretation of spurious peaks.

The validity of the proposed methodology is confirmed by the analyses of sediment cores taken from coastal cliffs at three different sites situated on the Nösse peninsula of the island Sylt. From the distributions of the two radiotracers within the cores, sedimentation rates in the order of 1 cm y$^{-1}$ were calculated. The $^{137}$Cs sedimentation model shows that at two of our study sites the tops of the cliffs are being denudated. For three of the four cores analyzed, $^{137}$Cs- and $^{210}$Pb-derived sedimentation rates are in close agreement. In these cores elevated fractions of coarse material correspond to periods of high sturm surge activity in this area. The results also indicate that sedimentation rates did not change within the last *ca.* 45 years, although an increase of storm surge activities has been documented for this time period. For one of the cores no reasonable geochronology could be established. As a consequence, we recommend to always take replicate samples from each site in any similar study.

## ACKNOWLEDGEMENTS

We wish to thank Belinde Stieve for taking the samples and for many fruitful discussions. The authors wish to acknowledge the assistance of Torsten Skubski and Dieter Wilkens in sample preparation. We thank Rüdiger Schmidt

for preparing the thin-sections and Werner Herzer for performing the γ-spectrometric analyses.

## LITERATURE CITED


ABRIL, J.M.; GARCIA-LEÓN, R.; SÁNCHEZ, C.I., and EL-DAOUSHY, F., 1992. Dating of marine sediments by an incomplete mixing model. *Journal Environmental Radioactivity*, 15, 135–151.

ACKERMANN, F.; BERGMANN, H., and SCHLEICHERT, U., 1983. Monitoring of heavy metals in coastal and estuarine sediments—a question of grain-size: <20 μm versus <60 μm. *Environmental Technology Letters*, 4, 317–328.

APPLEBY, P.G. and OLDFIELD, F., 1978. The calculation of lead-210 dates assuming a constant rate of supply of unsupported Pb-210 to the sediment. *Catena*, 5, 1–8.

BAUMANN, M., 1991. Die Ablagerung von Tschernobyl-Radiocäsium in der Norwegischen See und in der Nordsee. Ph.D. Dissertation. Universität Bremen, Fachbereich Geowissenschaften, Berichte, Nr. 14.

BENNINGER, L.K. and KRISHNASWAMI, S., 1981. Sedimentary processes in the inner New York Bight: evidence from excess $^{210}$Pb and $^{239,240}$Pu. *Earth Planetary Science Letter*, 53, 158–174.

BMU: BUNDESMINISTER FÜR UMWELT, NATURSCHUTZ UND REAKTORSICHERHEIT. *Umweltradioaktivität und Strahlenbelastung*. Bonn: Jahresberichte 1989–1992.

CADY, J.G.; WILDING, L.P., and DREES, L.R., 1986. Petrographic microscope techniques. *In:* Klute, A. (ed.), *Methods of Soil Analysis. Part 1: Physical and Mineralogical Methods* Madison: American Society of Agronomy, pp 185–218.

CHANTON, J.P.; MARTENS, C.S., and KIPPHUT, G.W., 1983. Lead-210 sediment geochronology in a changing coastal environment. *Geochimica Cosmochimica Acta*, 47, 1791–1804.

CUNDY, A.B. and CROUDACE, I.W., 1995. Physical and chemical associations of radionuclides and trace metals in estuarine sediments: an example from Poole Harbour, Southern England. *Journal Environmental Radioactivity*, 29, 191–211.

DELAUNE, R.D.; PATRICK, W.H.Jr., and BURESH, R.J., 1978. Sedimentation rates determined by $^{137}$Cs dating in a rapidly accreting salt marsh. *Nature*, 275, 532–533.

DIXON, W.J. (ed.), 1990. *BMDP Statistical Code Package*. 1990 Edition. Berkeley: University of California Press.

DOMINIK, J.; FÖRSTNER, U.; MANGINI, A., and REINECK, H.-E., 1978. $^{210}$Pb and $^{137}$Cs chronology of heavy metal pollution in a sediment core from the German Bight (North Sea). *Senckenbergiana Maritina*, 10, 213–227.

DUURSMA, E.K. and EISMA, D., 1973. Theoretical, experimental and field studies concerning reactions of radioisotopes with sediments and suspended particles of the sea. Part C. Applications to field studies. *Netherlands Journal Sea Research*, 6, 265–324.

EHLERS, J., 1988. *The Morphodynamics of the Wadden Sea*. Rotterdam: A. A. Balkema, 397p.

FRENCH, P.W.; ALLEN, J.R.L., and APPLEBY, P.G., 1994. 210-Lead dating of a modern period saltmarsh deposit from the Severn Estuary (Southwest Britain), and its implications. *Marine Geology*, 118, 327–334.

GEE, G.W. and BAUDER, J.W., 1986. Particle-size analysis. *In:* Klute A. (ed.), *Methods of Soil Analysis. Part 1: Physical and Mineralogical Methods* Madison: American Society of Agronomy, pp 383–411.

GOLDBERG, E.D. and KOIDE, M., 1962. Geochronological studies of deep sea sediments by the ionium/thorium method. *Geochimica Cosmochimics Acta*, 26, 417–450.

JAWOROWSKI, Z.; KOWNACKA, L.; GROTOWSKI, K., and KWIATKOWSKI, K., 1978. Lead-210 from nuclear explosions in the environment. *Nuclear Technology*, 37, 159–166.

KIRCHNER, G. and NOACK, C.C., 1988. Core history and nuclide inventory of the Chernobyl core at the time of the accident. *Nuclear Safety*, 28, 1–5.

KIRCHNER, G. and BAUMGARTNER, D., 1992. Migration rates of radionuclides deposited after the Chernobyl accident in various North German soils. *Analyst*, 117, 475–479.

KOIDE, M.; SOUTAR, A., and GOLDBERG, E.D., 1972. Marine geochronology with $^{210}$Pb. *Earth Planetary Science Letter*, 14, 442–446.

KRISHNASWAMY, S.; LAL, D.; MARTIN, J.M., and MEYBECK, M., 1971. Geochronology of lake sediments. *Earth Planetary Sciences Letter*, 11, 407–414.

LYNCH, J.C.; MERIWETHER, J.R.; MCKEE, B.A.; VERA-HERRERA, F., and TWILLEY, R.R., 1989. Recent accretion in mangrove ecosystems based on $^{137}$Cs and $^{210}$Pb. *Estuaries*, 12, 284–299.

MILAN, C.S.; SWENSON, E.M.; TURNER, R.E., and LEE, J.M., 1995. Assessment of the $^{137}$Cs method for estimating sediment accumulation rates: Louisiana salt marshes. *Journal Coastal Research*, 11, 296–307.

NIJAMPURKAR, V.N. and RAO, D.K., 1993. Polar fallout of radionuclides $^{32}$Si, $^{7}$Be and $^{210}$Pb and past accumulation rate of ice at Indian station, Dakshin Gangotri, East Antarctica. *Journal Environmental Radioactivity*, 21, 107–117.

OLSEN, C.R.; CUTSHALL, N.H., and LARSEN, I.L., 1982. Pollutant-particle associations and dynamics in coastal marine environments: a review. *Marine Chemistry*, 11, 501–533.

RANGARAJAN, C.; MADHAVAN, R., and GOPALAKRISHNAN, Smt.S., 1986. Spatial and temporal distribution of lead-210 in the surface layers of the atmosphere. *Journal Environmental Radioactivity*, 3, 23–33.

ROBBINS, J.A. and EDGINGTON, D.N., 1975. Determination of recent sedimentation rates in Lake Michigan using Pb-210 and Cs-137. *Geochimica Cosmochimica Acta*, 39, 285–304.

ROBBINS, J.A.; EDGINGTON, D.N., and KEMP, A.L.W., 1978. Comparative $^{210}$Pb, $^{137}$Cs, and pollen geochronologies of sediments from Lakes Ontario and Erie. *Quaternary Research*, 10, 256–278.

ROBBINS, J.A. and JASINSKI, A.W., 1995. Chernobyl fallout radionuclides in Lake Sniardwy, Poland. *Journal Environmental Radioactivity*, 26, 157–184.

SCHELL, W.R., 1977. Concentrations, physico-chemical states and mean residence times of $^{210}$Pb and $^{210}$Po in marine and estuarine waters. *Geochimica Cosmochimica Acta*, 41, 1019–1031.

*Stanners, D.A. and* ASTON, *S.R., 1981.* $^{134}$Cs:$^{137}$Cs and $^{106}$Ru:$^{137}$Cs ratios in intertidal sediments from the Cumbria and Lancashire coasts, England. *Estuarine Coastal Shelf Science*, 13, 409–417.

STÄBLEIN, G.; EHLERS, J., and STIEVE, B., 1993. Storm surges and their sedimentological record in salt marshes of the Wadden Sea; periodicity of a natural hazard. *In:* Smith, D.E. (ed.), *Climate Change, Sea Level Rise and Associated Impacts in Europe*. Final Report of work undertaken for the Commission of the European Communities under contract EPOC-CT90-0015.

STILLER, M. and IMBODEN, D.M., 1986. $^{210}$Pb in Lake Kinneret waters and sediments: residence times and fluxes. *In:* Sly P.G. (ed.), *Sediments and Water Interactions*. New York: Springer, pp 501–511.

TUREKIAN, K.K.; NOZAKI, Y., and BENNINGER, L.K., 1977. Geochemistry of atmospheric radon and radon products. *Annual Reviews Earth Planetary Science*, 5, 227–255.